

The Development of 460 GHz gyrotrons for 700 MHz DNP-NMR spectroscopy

T. Idehara · Y. Tatematsu · Y. Yamaguchi ·
E. M. Khutoryan · A. N. Kuleshov · K. Ueda ·
Y. Matsuki · T. Fujiwara

Received: 2 December 2014 / Accepted: 20 February 2015 /
Published online: 15 March 2015
© Springer Science+Business Media New York 2015

Abstract Two demountable gyrotrons with internal mode converters were developed as sub-THz radiation sources for 700 MHz DNP (Dynamic Nuclear Polarization) enhanced NMR spectroscopy. Experimental study on the DNP-NMR spectroscopy will be carried out in Osaka University, Institute for Protein Research, as a collaboration with FIR UF. Both gyrotrons operate near 460 GHz and the output CW power measured at the end of transmission system made by circular waveguides is typically 20 to 30 watts. One of them named Gyrotron FU CW GVI (we are using “Gyrotron FU CW GO-1” as an official name in Osaka University) is designed to have a special function of high speed frequency modulation δf within 100 MHz band. This will expand excitable band width of ESR and increase the number of electron spins contributing to DNP. The other gyrotron, Gyrotron FU CW GVIA (“Gyrotron FU CW GO-II”) has a function of frequency tunability Δf in the range of wider than 1.5 GHz, which is achieved in steady state by changing magnetic field intensity. This function should be used for adjusting the output frequency at the optimal value to achieve the highest enhancement factor of DNP.

Keywords Gyrotron · Second harmonic · DNP · NMR · sub THz · Frequency modulation · Frequency tunability

T. Idehara (✉) · Y. Tatematsu · Y. Yamaguchi · E. M. Khutoryan · A. N. Kuleshov
Research Center for Development of Far-Infrared Region, University of Fukui (FIR UF), Bunkyo 3-9-1,
Fukui-shi, Fukui-ken 910-8507, Japan
e-mail: idehara@fir.u-fukui.ac.jp

T. Idehara
Gyro Tech Co. Ltd., Keya 3-2-4, Fukui-shi, Fukui-ken 918-8550, Japan

E. M. Khutoryan · A. N. Kuleshov
O. Ya. Usikov Institute for Radiophysics and Electronics IRE NASU, 12,ac. Proskura str., Kharkiv 61085,
Ukraine

A. N. Kuleshov · K. Ueda · Y. Matsuki · T. Fujiwara
Institute for Protein Research, Osaka University, Yamada-oka 3-2, Suita-shi, Osaka-fu 565-0871, Japan

1 Introduction

In the past three decades, high frequency gyrotrons [1–5] using high magnetic field and high harmonic operations were developed for applications to not only heating of fusion plasmas [6] but also many high power THz technologies [7] including high power THz spectroscopy [8–15] and material processing [16, 17]. Some of these gyrotrons have achieved the breakthrough of 1 THz in both pulse [18, 19] and CW operation modes [20]. The output power of them are not so high, typically 100 W to several kW [21]. However, these powers are still quite high in THz region comparing with other radiation sources, both vacuum devices and solid state radiation sources. Especially, in a recent decade, many active spectroscopy using high power THz radiation sources – “Harmonic Gyrotrons” [21] were advanced. Great capability of the high frequency gyrotrons were confirmed by many applications opened only by high power THz radiation sources. For such objectives of gyrotrons, we have begun the development of high frequency, harmonic gyrotrons and their applications in University of Fukui in early 1980s [21].

After then, we have leaded this research area in the world. At the first step, we have developed Gyrotron FU Series including 9 gyrotrons with pulse operation and applied them to plasma diagnostics on scattering measurement of drift waves [13] and high frequency ESR spectroscopy [14]. In 1990s, we have developed Gyrotron FU CW Series which consists of more than fifteen CW gyrotrons and applied them to many high power THz technologies – including DNP-NMR spectroscopy [8–11], ESR echo experiment, X-ray detected magnetic resonance (XDMR) experiment [15], new medical technology for cancer treatment by use of hyperthermia [22, 23] and material processing [16, 17] by use of heating effect of THz radiation. Among them, for DNP-NMR spectroscopy, we have already developed 7 gyrotrons [24] included in Gyrotron FU CW Series and successfully applied to sensitivity enhancement of 200 MHz, 300 MHz and 600 MHz [9] NMR spectrometers. On the basis of such many successes, we have just begun the development of 460 GHz gyrotrons for the highest frequency DNP-NMR spectroscopy at 700 MHz. In this paper, we will present the design, construction, operation test and the results of two 460 GHz gyrotrons named Gyrotrons FU CW GVI and GVIA. These were developed as the latest gyrotrons included in Gyrotron FU CW G series which consists of gyrotrons with mode converter system for Gaussian mode output and designed on the basis of the successful operation results of Gyrotrons FU CW GI [25], FU CW GII [26, 27] and FU CW GIII [27, 28].

In the next section, the design of both Gyrotrons FU CW GVI and GVIA is presented. In the third and fourth sections, the operation test results of both gyrotrons are presented and in the final section, a summary and the future prospects are presented briefly.

2 Design of Gyrotron FU CW GVI and GVIA

Each gyrotron consists of a demountable tube, a 10T superconducting magnet with refrigerator for cooling down the magnet to around 4K and high voltage power supply systems for electron gun. The designs of both gyrotron tubes are basically same except for the longer cavity for the gyrotron FU CW GVIA for making the frequency tunable range wider. The internal mode converter is installed for each gyrotron. Therefore, the output power can be extracted by Gaussian beam. In Fig. 1, the cross section of Gyrotron FU CW GVI is illustrated. A gyrotron tube with internal mode converter is installed on the axis of a 10 T superconducting magnet. Gyrotron FU CW GVIA is almost same construction as the FU CW GVI. The power supplies for acceleration voltage of electrons and the anode voltage are Spellman’s and Trek Japan Co.’s products. The superconducting magnet is a JAS TEC’s 10 T magnet. In Table 1, main

parameters of both gyrotrons are summarized. As already mentioned, FU CW GVI is designed to have a special function of frequency modulation. The amplitude is around 100 MHz with a modulation speed of up to 10 kHz. This function is quite important, because it expands the excitation width ESR and the number of electron spins contributing to DNP is increased around ten times in a static sample condition. As the results, the sensitivity of NMR spectroscopy will be significantly enhanced. The second gyrotron FU CW GVIA has another function of frequency tunability for adjusting the output frequency at the optimal condition for DNP. The tuning range should be 1.5 GHz. By applying both functions, the DNP enhancement factor will be improved significantly. Although it is known that the DNP efficiency is decreased at higher field conditions, the gain from the frequency modulation could compensate it.

After long term operation training (totally more than one hundred hours) and achieving the stable operation, we have tried to measure the operation characteristics of both gyrotrons. The vacuum in the tube is in quite good condition, the pressure is less than 6×10^{-6} Pa.

3 Operation test results of Gyrotron FU CW GVI

3.1 Confirmation of the operation at the designed cavity mode

First of all, we tried to confirm if the operation cavity mode is TE_{8,5} at 460.4 GHz. The measurement of output frequency using heterodyne detection system which consists of the Agilent's Analog Signal Generator (E8257D) as a local oscillator, the Agilent's Spectrum Analyzer (CSA NT996A) and the Virginia Diode's Harmonic Mixer (WR-2.2EHM). The measured frequency is 460.82 GHz at the operation conditions set as follows; the field intensity: 8.5 T, the cathode voltage: -14 kV, the anode voltage: -8 kV, the beam current: 120 mA. Observed mode patterns are elliptical and the angle of the emission is almost horizontal, after four mirrors of the mode converter system are installed at the designed angles. The beam is emitted a little bit up-ward. We improved the angle of the fourth mirror, so that the beam emits horizontally. We could confirm the operation cavity mode is the designed mode TE_{8,5} because the measured frequency is quite close to the designed one and, in addition, the emission angle of the output beam is almost following the designed arrangement of the mode converter system.

3.2 Output power as functions of magnetic field intensity

The output power from Gyrotron FU CW GVI is measured by use of a pyro-electric detector with a chopper. A CW power can be measured by such a way by use of a chopper.

Table 2 and Fig. 2 demonstrate the measurement and calculation results. Here, the measured output power is shown as a function of the magnetic field intensity. The vertical axis is in arbitrary unit. Structure factor $\chi = \frac{J_{m-n}^2(kR_e)}{((kR_e)^2 - m^2) J_m^2(kR_e)}$ shows level of beam-wave coupling. Here J_p is the Bessel function of p^{th} order, m is azimuthal order of the mode, n is harmonic number, R_e and R_c are electron beam and cavity radius.

The calculations have been carried out with the self-consistent formalism [29]. The accuracy of the measurement of field intensity made by the industry is within ± 1 percent. Agreement between measured and calculated results is fairly good if shifting the field intensity by -0.27 percent from the measurement result. The higher peaks seen at the right hand side are corresponding to the fundamental operations at TE_{4,3}, TE_{7,2}, TE_{2,4} and TE_{0,4}. The last peak

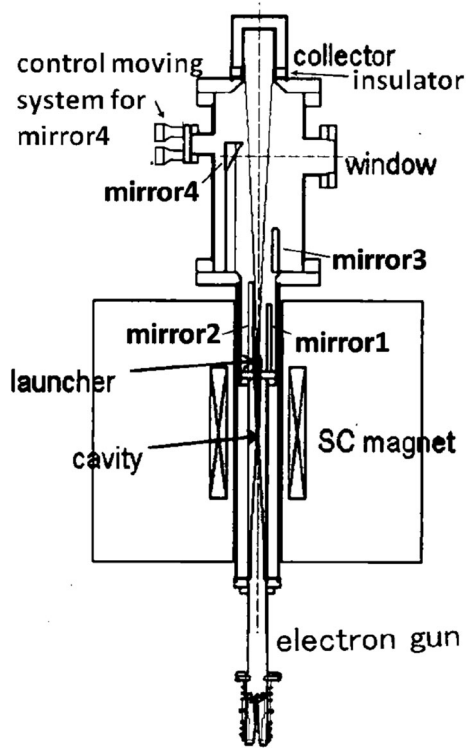


Fig. 1 The cross-section of gyrotron FU CW GVI

Table 1 Designed parameters of two 460 GHz gyrotrons operating at the second harmonic resonance

Gyrotron number	Gyrotron FU CW GVI	Gyrotron FU CW GVIA
Gyrotron tube	Demountable	Demountable
Frequency f	460.4 GHz	459–461 GHz
Frequency modulation δf	200 MHz	–
Frequency tunability Δf	–	1.5 GHz
Output power P	>30 W	>20 W
Beam energy V_b	20 keV	20 keV
Pitch factor α	1.2	1.2
Cavity diameter d_c	5.098 mm	5.098 mm
Cavity length L_c	15 mm	20 mm
Cavity mode	TE _{8,5}	TE _{8,5}
Magnet type	10T SC magnet	10T SC magnet
Intensity at cavity B_c	8.55 T	8.55 T
Electron gun	Triode MIG	Triode MIG
Intensity at gun B_1	0.2 T (Max)	0.2 T (Max)
Operation mode	CW and pulsed	CW and pulsed

is including two modes $TE_{2,4}$ (excited at lower magnetic field) and $TE_{0,4}$. The other three lower peaks are corresponding to the second harmonic operations at $TE_{1,8}$, $TE_{8,5}$ and $TE_{11,4}$. The designed mode $TE_{8,5}$ is seen at a little bit lower field intensity than 8.5 T. The operation conditions of the gyrotron are as follows; the acceleration voltage U_c : 16 kV, the anode voltage U_a : 9 kV and the electron beam current I_b : typically 220 mA. In the next step, we tried to measure the absolute output power by use of a water load. The measurement is carried out at the end of a waveguide system. It consists of a taper waveguide for converting the output power beam from the window to the circular waveguide mode, four straight circular waveguides and three miter bends. A power loss during transmission through four straight waveguides and three miter bends is measured. It is around 4 dB. Therefore, the output power at the window is higher than the measurement results shown in Fig. 3 by more than twice. The measurement results are shown in Fig. 3. In the figure, the measured power is shown as functions of magnetic field intensity. The parameter is an acceleration voltage U_c . It is seen the field intensity corresponding to the peak power shifts to higher field with increased U_c . This is reasonable with the rough estimation results.

One can see that there are oscillations for magnetic field values lower than designed ones. We confirmed that they are due to excitation of $TE_{1,8,q}$ modes and correspond to frequency lower than 457 GHz. The highest power measured for $TE_{8,5,1}$ is around 30 W in CW operation mode. This means the power at the window is higher than 60 W. In addition, the field range where the output power is higher than 5 W is quite wide. Let us notice that results shown in Fig. 3 obtained with the beam current almost twice lower than maximal designed one. Therefore, we can expect the frequency tunable range will be quite wide and adjust the frequency of the gyrotron at the optimal condition for DNP-NMR spectroscopy easily by only adjusting the field intensity B or the acceleration voltage U_c .

3.3 Frequency as functions of magnetic field intensity

Next, we have carried out frequency measurement using the heterodyne system, which is presented in detail in sub-session III-1. Fig. 4 demonstrates the frequency spectrum of IF signal measured by the heterodyne system. The parameters of the system are set as follows; the center frequency of the spectrum analyzer f_0 : +1 GHz, the frequency of the local oscillator f_L : 38.2929 GHz, the harmonic number of the mixer n : 12. Then, we can estimate the frequency of the gyrotron output: f as $f = nf_L + f_0$. We have obtained the frequency as $f = 460.515$ GHz. From the shape of the observed spectrum in Fig. 4, the half value width is less than 3 MHz. In such a

Table 2 Parameters of the gyrotron: cut-off frequency, resonance cyclotron field intensity, magnetic intensity at experimentally obtained generation, structure factor and calculated minimal starting current

Mode	$f_{cut-off}$ GHz	$B_{cycl-res}$, T	B_{exper} , T	χ	I_{st-min} , mA
$TE_{1,8}$	455.08	8.38	8.33-8.38	0.007	45
$TE_{8,5}$	460.25	8.475	8.44-8.47	0.007	47
$TE_{11,4}$	468.13	8.62	8.6-8.62	0.007	44
$TE_{4,3}$	237.389	8.743	8.63-8.73	0.022	16
$TE_{11,1}$	240.095	8.843		0.0	>300
$TE_{7,2}$	242.077	8.916	8.8-8.93	0.001	170
$TE_{2,4}$	246.532	9.08	8.93-9.1	0.011	30
$TE_{0,4}$	249.402	9.186	9.1-9.18	0.011	28

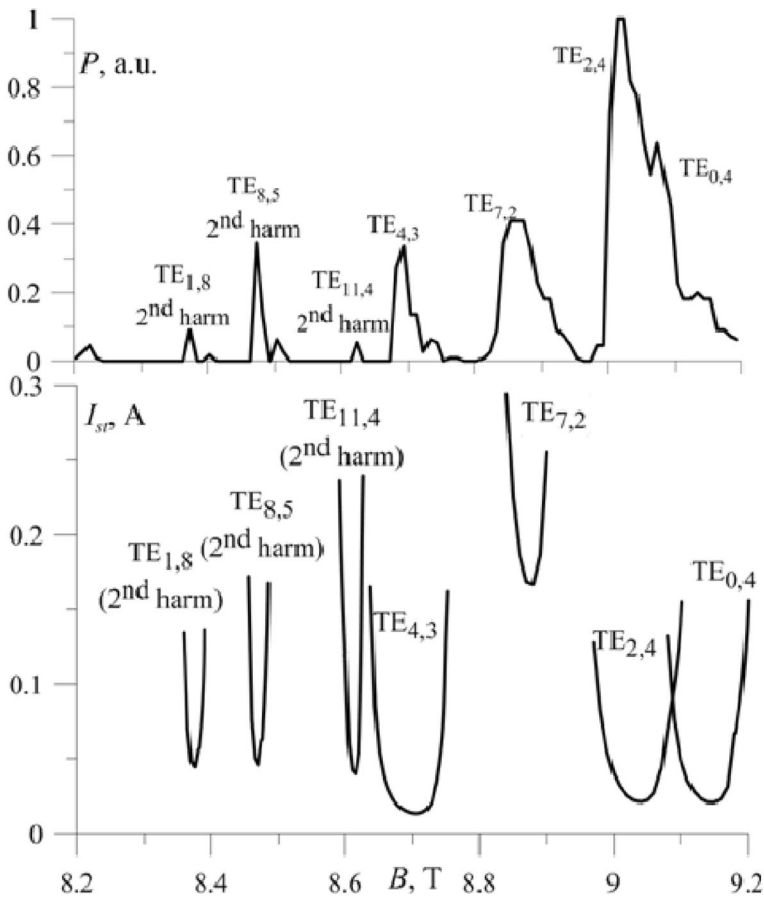


Fig. 2 Output power (upper) measured by a pyro-electric detector and calculated starting current (lower) as a function of magnetic field intensity B . At calculations $R_c=0.934$ mm, $\alpha=1.4$

way, we have measured output frequency f as a function of magnetic field intensity B . The results are shown in Fig. 5 for $I_b = 280$ mA. Such beam current provides excitation of higher axial modes $TE_{8,5,q}$ with output power higher than 1 W almost in all measured points shown on Fig. 5. As shown in this figure, the frequency changed in wide range of around 0.65 GHz (from 460.30 GHz to 460.95 GHz) even in the short cavity case, when the field intensity changed from 8.485 T to 8.540 T. In the lower part of Fig. 5, the measured frequencies are shown with the calculated frequency at the starting current (the solid line). The calculated frequency is fairly good agreement with the measurement results, by shifting the field intensity by -0.27 percent from the measurement result. In the upper figure, the calculated starting current I_{st} is demonstrated as a function of the field intensity. Comparison with the frequency measurement suggests that higher axial modes up to third ($q=3$) are contributing to the frequency tunability. Because, we can shift reasonably the field intensity by -0.27 percent like the similar situation indicated elsewhere [28].

We can use the frequency tunability in wide range for adjusting the frequency at the optimal condition of DNP and achieve the highest enhancement factor of NMR sensitivity. In addition, we can achieve the frequency quick modulation by the modulation of the energy of beam

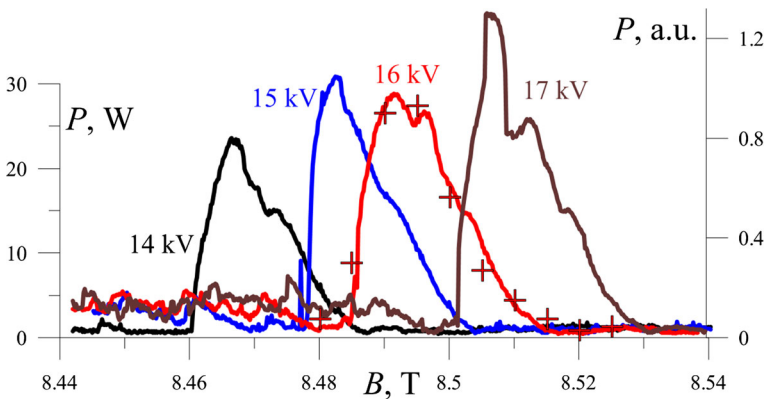


Fig. 3 Output power measured by a water load (points+) and pyroelectric detector with a chopper (lines) as functions of magnetic field intensity for various acceleration voltages U_c . Beam current I_b : 220 mA

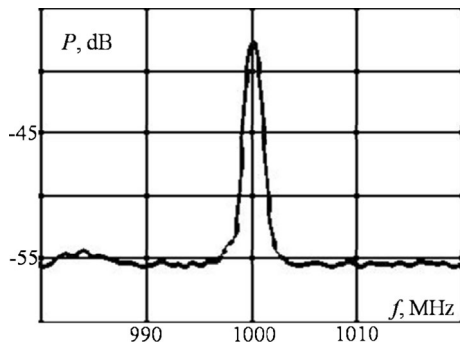
electrons which is realized by modulation of the body potential, because the modulation of beam energy is equivalent to modulation of field intensity. The feasibility has previously been demonstrated by use with of gyrotron VI, where we have succeeded in frequency modulation amplitude of 40 MHz [30].

3.4 Measurement of emission patterns

The output power from the cavity end is converted by the mode conversion system into the Gaussian-like beam. The conversion system consists of a helical cut launcher and four mirrors.

The system emits the radiation finally through the center of the window. After emitted from the window, we tried to measure the patterns of the emission (the distribution of radiation power on the surface put parallel to the window surface). The distribution of the power can be measured as the temperature increase on the polymer sheet irradiated by the radiation. We used PCV polymer sheet with 1 mm thickness. Gyrotron operation was in CW mode. Typically irradiating time of polymer sheet was 3–5 sec (the time was chosen in such way that the highest temperature was always lower than 80° C). Fig. 6 demonstrates the measured distribution of temperature increase with the distance Z_p between the window surface and the polymer sheet as a parameter. In Fig. 6, the measured emission patterns observed on the polymer sheet are shown with the distance Z_p as a parameter. An infrared camera is used for the measurement on distribution of temperature increase. The location of the camera is fixed at 85 cm from the

Fig. 4 Frequency spectrum of IF signal. The center frequency f_0 : 1 GHz, one division of horizontal axis: 10 MHz, the frequency of local oscillator 38.2929 GHz, harmonic number: 12



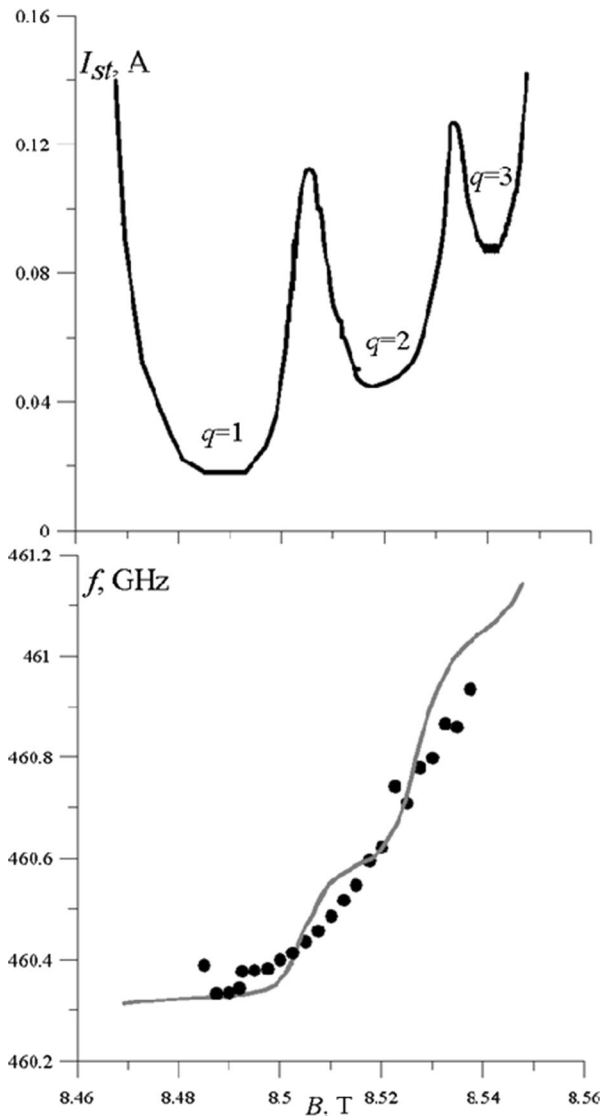


Fig. 5 Upper: the calculated starting current I_{st} for $R_e=0.71$ mm. Lower: Frequency measurement results with the calculation result at the starting current. The acceleration voltage U_c : 16 kV, beam current I_b : 280 mA

window surface in the microwave beam direction. When the position of the polymer sheet is changed from 10 cm to 60 cm, the distance between a camera and a polymer sheet is also changed. Therefore, we should make a correction of the scale on each figure coming from the difference of the distance between a camera and a polymer sheet. As seen in the figure, in this case also, the radiation beam does not propagate in the direction accurately perpendicular to the window surface. At the distance $Z_p=50$ cm, the discrepancy on the measured emission patterns on the Fig. 6 is at most 2 cm. The angle deviation from the vertical direction to the window is at most 1.3 degree. Such small deviation of the angle can be corrected by the special design of the quasi-optical transmission system using the measurement results of the emission patterns.

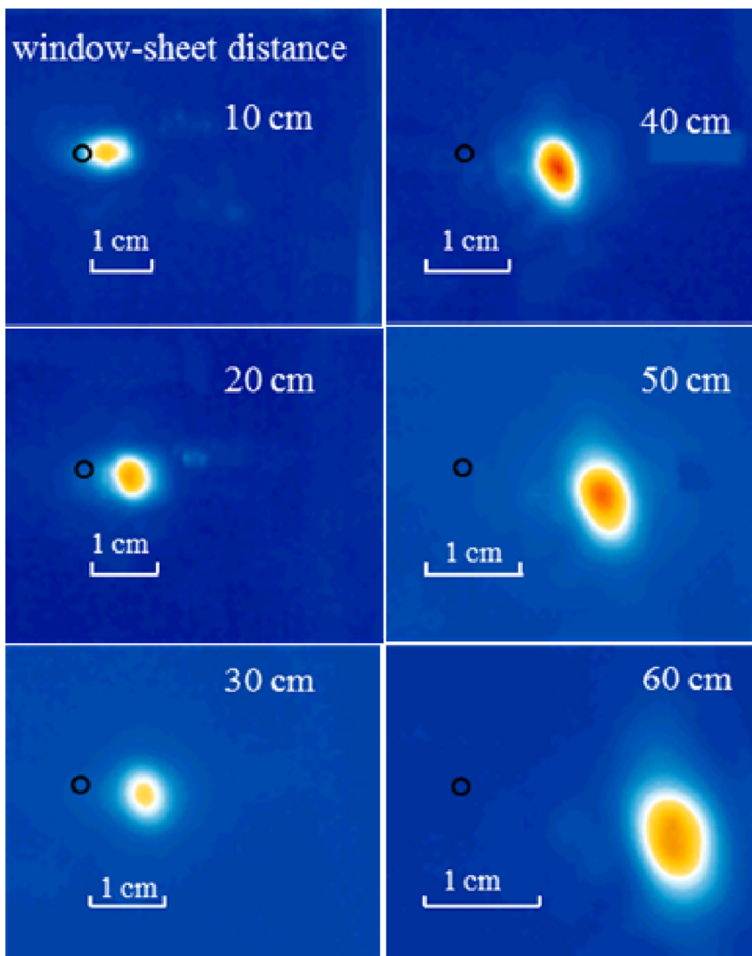


Fig. 6 Emission patterns with the distance of Z_p as a parameter. Here, the acceleration voltage U_c : 14 kV

4 Operation test results of Gyrotron FU CW GVIA

In the case of Gyrotron FU CW GVIA, the concept of the design is the same as FU CW GVI gyrotron. However, the fabrication errors of cavity diameters are a little bit different. This makes the operation characteristics different. Therefore, we will summarize the operation test results for FU CW GVIA gyrotron briefly, in the similar way to the previous gyrotron.

4.1 Confirmation of the operation at the designed cavity mode

At first, we have measured the output frequency in order to confirm the operation cavity mode. We used the same heterodyne system. The measured frequency is 459.526 GHz at the operation conditions set as follows; the field intensity: 8.4501 T, the acceleration voltage: 14.24 kV, the anode voltage: 8.58 kV, the beam current: 236 mA. The measured frequency is included in the designed tunable frequency range (from 459 GHz to 461 GHz). In addition, the radiation from the end of cavity is converted well into Gaussian like beam and emitted through

the center of the window when the mode convertor arrangement is adjusted at the designed formation. The emission direction is almost horizontal. We could not find any deviation from the designed performance. This fact may partially support the operating cavity mode is designed mode $TE_{8,5}$.

4.2 Output power as functions of magnetic field intensity

Next, the output power is measured as functions of magnetic field intensity B with the acceleration voltage U_c as a parameter. The measurement results are shown in Fig. 7. The output power is measured by use of a water load installed at the end of the same circular waveguide system as we used for measurement on FU CW GVI gyrotron. As looked in the figure, the maximum power observed at the field intensity corresponding to the top of each curve is around 16 W in CW operation mode. Considering the power loss in the transmission system is 4 dB, the output power at the window is higher than 35 W. The output power at the window should be higher than 5 W, if we will apply it for DNP-NMR spectroscopy. Such range in the magnetic field intensity is quite wide. This means we can expect fairly wide frequency range for application to DNP enhancement of NMR sensitivity. When the acceleration voltage U_c is increased, the field intensity corresponding to the maximum power shifts to higher field. This feature is the same as the case of FU CW GVI gyrotron as shown in Fig. 3.

4.3 Frequency as functions of magnetic field intensity

The measurement results of output frequency are shown in Fig. 8. The acceleration voltage U_c is 19 kV. These oscillations correspond to $TE_{8,5,q}$ mode. We confirmed that for magnetic field higher than 8.63 T the $TE_{11,4}$ mode is excited ($f > 467.9$ GHz); for lower than 8.5 T the $TE_{1,8}$ mode is excited ($f < 458$ GHz). The tuning range of output frequency for $TE_{8,5}$ mode is fairly wide, around 4 GHz. As one can see the lowest observed frequency was about 0.7 GHz lower than cut off of $TE_{8,5}$ mode at designed cavity diameter. This can be explained by cavity diameter fabrication error of about 10 μm . The solid line in Fig. 8 is a calculation result of the output frequency at the starting current I_{sr} . Such a wide tuning range can be achieved by the longer length of the cavity (the length of the cavity of FU CW GVIA gyrotron is 20 mm). Corresponding output power was measured by both a water load and a pyro electric detector with a chopper. The results are shown in Fig. 9. In the figure, a solid line shows the results of a pyro electric detector and squares show the results of a water load. These measurements are

Fig. 7 Output power measured by a water load (points+) and pyro-electric detector (lines) as functions of magnetic field intensity. U_c is a parameter

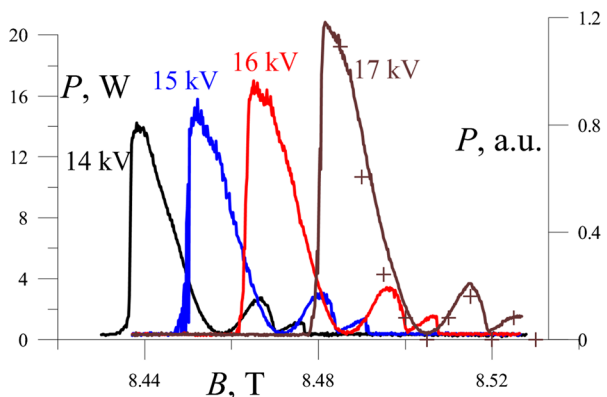
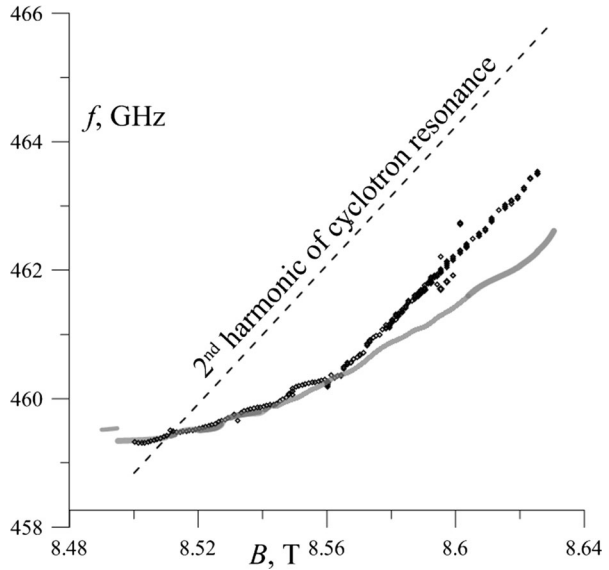


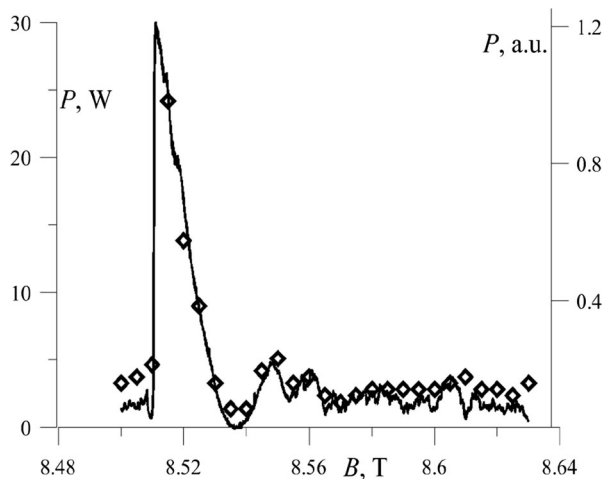
Fig. 8 Measured and calculated frequencies as a function of a magnetic field intensity B . $U_c = 19$ kV



carried out at the end of the waveguide system. The real power at the output window should be multiplied by 2.5. Therefore, the frequency tuning range is extended in wide range keeping the output power of 5 W at the window. We can adjust frequencies of both gyrotrons at the optimum conditions for DNP simultaneously at each of two maxima of enhancement factor. This means that the enhancement factor will be increased even in high frequency NMR at 700 MHz, overcoming decrease of the enhancement factor inversely proportional to the NMR frequency.

If we will need to extend the tuning range wider, we are preparing the alternative way, that is, changing the resonant cavities with different diameters in order to change the center frequency. We have some experiences for this way for the frequency change using Gyrotron FU CW GI [31] and this is one of most important advantages of the demountable gyrotron tubes.

Fig. 9 Measured power as a function f of magnetic field intensity B . $U_c = 19$ kV. Squares are powers measured by a water load



4.4 Measurement of emission pattern

Emission patterns from the window of FU CW GVIA gyrotron are measured at the several points on the front of the window by use of a polymer sheet and an infrared camera. As mentioned in the previous section, the distribution of the radiation intensity is measured as the temperature increase on the polymer sheet irradiated by radiation from the window. Fig. 10 shows the patterns of temperature increase with the distance between the window surface and the polymer sheet as a parameter. The shape of the pattern indicates the emitted beam is Gaussian-like. The location of the infrared camera is fixed at the distance from the window of 70 cm. For each pattern, we should correct the scale by considering difference in the distance between a camera and a polymer sheet. In this case also, the direction of the emitted beam is not accurately perpendicular to the window surface, because the pattern moves to left hand side, when it propagates. However, a propagation angle from the vertical direction is quite small, it is less than 1 degree. Such a small deviation in the propagation angle can be corrected by the special design of the quasi-optical transmission system, which will be supplied by Bridge 12 Technologies, Inc.

5 Summary and future prospects

On the basis of the long term experiences on the development of high frequency gyrotrons for application to DNP-NMR spectroscopy at Osaka University, University of Warwick and our research center (FIR Center) in University of Fukui, we have developed two new gyrotrons for

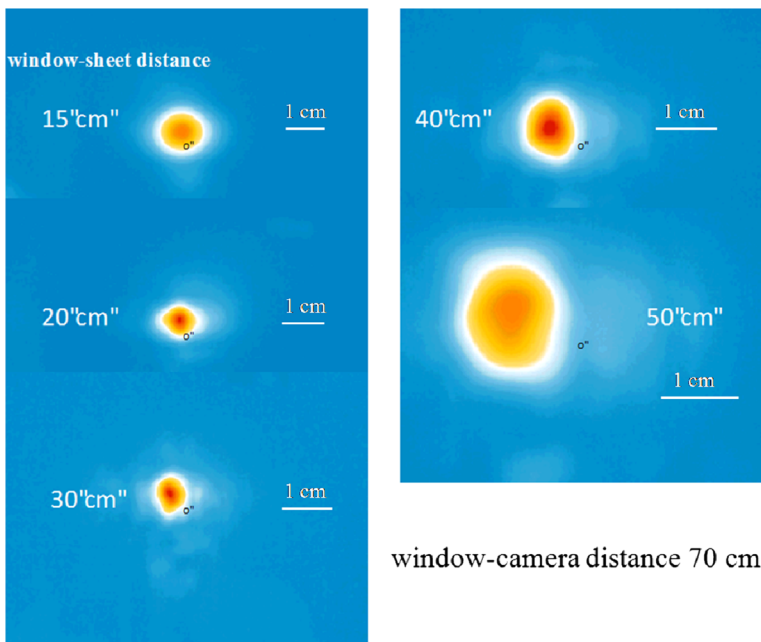


Fig. 10 Emission pattern measured on the polymer sheet as the temperature increase. The distance from window is a parameter

700 MHz DNP-NMR spectroscopy to realize the sensitivity enhancement for application to analysis on the structure of complicated protein molecule. After construction of both gyrotrons named FU CW GVI (called officially in Osaka University as “Gyrotron FU CW GO-I”) and GVIA (as “Gyrotron FU CW GO-II”), we have successfully carried out the operation tests of them. The results are summarized as follows,

- 1) At first, from the measurement of the output frequency at the conditions closed to designed parameters, we could confirm the operation cavity mode is the designed mode $TE_{8,5}$ at the second harmonic resonance. The measured frequency of 460.82 GHz is quite close to the designed frequency 460.4 GHz
- 2) The measurement results of the output power as a function of magnetic field intensity shows both gyrotrons demonstrate three second harmonic modes and four fundamental modes near the designed magnetic field intensity of 8.55 T. One of second harmonic modes is identified as the designed mode $TE_{8,5}$. The power reaches around 60 W in CW operation and the magnetic field intensity range where the output power exceeds 5 W is quite wide.
- 3) As seen in the measurement of output frequency, both gyrotrons have achieved the frequency continuous tunability in fairly wide range of around 1 GHz to 4 GHz. Such a wide frequency tunability can be applied to DNP enhanced NMR spectroscopy in order to adjust the frequency of gyrotron at the optimal condition of the DNP. As known well, a gyrotron is essentially a frequency-fixed radiation source. A frequency wide tunability realized is possibly considered as the result of higher axial mode operations, which has been confirmed by both experiment and following theoretical consideration with non-fixed structure of RF field in the cavity [28, 32].
- 4) Measurement of the emission patterns is carried out by measuring the temperature increase on the polymer sheet irradiated by the gyrotron output power. The patterns obtained as photos of an infrared camera indicate the emission patterns are Gaussian-like. The propagation direction of the radiation beam is not accurately perpendicular to the window surface. But, the deviation angle from the perpendicular direction is only 1~2 degree or less. Such a small deviation of the emission direction can be corrected by the specially designed quasi-optical transmission system.

These gyrotrons will be used for 700 MHz DNP-NMR spectrometer installed at Osaka University, Institute for Protein Research. Before the application, the output power with Gaussian-like emission pattern will be transmitted by a quasi-optical transmission system designed and supplied by Bridge 12 Technologies, Inc. Finally, the radiation from both gyrotrons is merged into the single beam and irradiated on the sample installed in the 700 MHz NMR spectrometer.

In addition, the gyrotrons should operate in stable state so long term up to several hours or some times several days for measurement on complicated protein molecule, etc. Therefore, we need to stabilize the output power by use of a PID control system for the feedback control of a beam current and an anode voltage of electron gun. We have already succeeded in the experiment for long-term power stabilization up to more than 10 hours [33] using Gyrotron FU CW IIB.

We need also to modulate the output frequency of the first gyrotron (FU CW GVI) for extending the number of electron spins contributing to DNP and then increase the enhancement factor significantly.

After overcoming such many challenging trials, we hope the first measurement on high sensitive NMR spectroscopy at 700 MHz with DNP enhancement will be carried out soon.

Acknowledgements This work was partially supported by Grant in Aid for Scientific Research (B) (No. 25630142) from Japan Society for Promotion of Science (JSPS) and SENTAN project of JST. This work was performed under the Cooperative Research Program of Institute for Protein Research, Osaka University.

References

1. M. Thumm, State-of-the-Art of High Power Gyro-Devices and Free Electron Masers, KIT Scientific Reports 7662 (2013).
2. S.E. Spira-Hakkarainen, K.E. Kreischer, R.J. Temkin, Submillimeter-wave harmonic gyrotron experiment, *IEEE Trans. Plasma Science*, PS-18, 334-342 (1990).
3. T. Idehara, T. Tatsukawa, I. Ogawa, H. Tanabe, T. Mori, S. Wada and T. Kanemaki, Development of a second cyclotron harmonic gyrotron operating at 0.8 mm wavelength, *Appl. Phys. Letts.* 56, 1743-1745 (1990).
4. V.A. Flyagin, A.G. Luchinin, G.S. Nusinovich, Submillimeter wave gyrotrons theory and experiment, *Int. J. Infrared and Millimeter Waves* 4, 629-637 (1983).
5. G.F. Brand, P.W. Fekete, K. Hong, K.J. Moore and T. Idehara, Operation of a tunable gyrotron at the second harmonic of the electron cyclotron frequency, *Int. J. Electronics* 68, 1099-1111 (1990).
6. M. Thumm, Progress on gyrotrons for ITER and future thermonuclear fusion reactor, *IEEE Trans. On Plasma Science* 39, 971-979 (2011).
7. T. Idehara, S.P. Sabchevski, Development and applications of high-frequency gyrotrons in FIR FU covering the sub-THz to THz range, *J. Infrared, Millimeter and Terahertz Waves* 33 667-694 (2012).
8. V.S. Bajaj, C.T. Farrar, M.K. Hornstein, I. Mostovsky, J. Vieregg, J. Bryant, B. Elena, K.E. Kreischer, R.J. Temkin, R.G. Griffin, Dynamic nuclear polarization at 9 T using anovel 250 GHz gyrotron microwave source, *J. Magnetic Resonance* 160, 85-90 (2003).
9. Yoh Matsuki, Keisuke Ueda, Toshitaka Idehara, Ryosuke Ikeda, Isamu Ogawa, Shinji Nakamura, Mitsuru Toda, Takahiro Anai, Toshimichi Fujiwara, Helium-cooling and -spinning dynamic nuclear polarization for sensitivity-enhanced solid-state NMR at 14 T and 30 K, *Journal of Magnetic Resonance* 225, 1-9 (2012).
10. Kevin J. Pike, Thomas F. Kemp, Hiroki Takahashi, Robert Day, Andrew P. Howes, Eugeny V. Kryukov, James F. MacDonald, Alana E.C. Collis, David R. Bolton, Richard J. Wylde, Marcella Orwick, Kosuke Kosuga, Andrew J. Clark, Toshitaka Idehara, Anthony Watts, Graham M. Smith, Mark E. Newton, Ray Dupree, Mark E. Smith, A spectrometer designed for 6.7 and 14.1 T DNP-enhanced solid-state MAS NMR using quasi-optical microwave transmission, *Journal of Magnetic Resonance* 215, 1-9 (2012).
11. S. Alberti, J. Ph. Ansermet, F. Braunmuller, P. Cuanillon, J. Dubray, D. Fasel, J. Ph. Hogge, A. Macor, E. de Rijk, M.Q. Tran, T.M. Tran, Q. Vuillemin, Experimental results on a modular gyrotron operating at 0.26 THz for 400 MHz DNP/NMR spectroscopy application, 38th Int. Conf. on Infrared. Millimeter and Terahertz Waves (IRMMW-THz 2012), Wollongong, Australia, Sept 23-28, 2012, Thu-A-3.
12. T. Yamazaki, A. Miyazaki, T. Suehara, T. Namba, S. Asai, T. Kobayashi, H. Saito, I. Ogawa, T. Idehara, S. Sabchevski. Ditect observation of the hyperfine transition of ground-state positronium, *Phys. Rev. Letts.* 108, 253401-5 (2012).
13. I. Ogawa, M. Iwata, T. Idehara, K. Kawahata, H. Iguchi, A. Ejiri, Plasma Scattering Measurement using a submillimeter wave gyrotron (Gyrotron FU II) as a power source, *FusionEngineering and Design*, 34-35, 455-458 (1997).
14. T. Tatsukawa, T. Maeda, H. Sasai, T. Idehara, M. Mekata, T. Saito and T. Kanemaki, ESR spectrometer with a wide frequency range using a gyrotron as aradiation power source, *Int. J. Infrared Millimeter Waves* 16, 293-305 (1995).
15. A. Rogalev, J. Goulon, G. Goujon, F. Wilhelm, I. Ogawa and T. Idehara, X-ray detected magnetic resonance at sub-THz frequencies using a high power gyrotron, *J. Infrared, Millimeter and Terahertz Waves* 33, 777-793 (2012).
16. Y. Bykov, A.F.L. Goldenberg, V. A. Flyagin, The possibilities of material processing by intense millimeter-wave radiation, *Mat. Res. Soc. Symp. Proc.*, 169, 41-42 (1991).
17. T. Kikunaga, H. Asano, Y. Yasojima, F. Sato, T. Tsukamoto, A 28 GHz gyrotron with a permanent magnet system, *Int. J. Electronics*, 79, 655-663 (1995).
18. T. Idehara, H. Tsuchiya, O. Watanabe, La Agusu and S.Mitsudo, The first experiment of a THz gyrotron with a pulse magnet, *Int. J. Infrared and Millimeter Waves* 27, 319-331 (2006).
19. M. Yu. Glyavin, A.G. Luchinin, G. Yu. Golubiatnikov, Generation of 1.5-kW, 1 THz coherent radiation from a gyrotron with a pulsed magnetic field, *Phys. Rev. Letts.* 100, 015101-1~015102-3 (2008).

20. O. Watanabe, H. Tsuchiya, H. Mori, La Agusu, S. Mitsudo, I. Ogawa, T. Saito, T. Idehara, Development of a Tera Hertz Gyrotron as a Radiation Source, *Plasma and Fusion Research: Rapid Communications* 2, 024 (2007).
21. T. Idehara, T. Tatsukawa, I. Ogawa, Y. Shimizu, N. Nishida and K. Yoshida, Development and applications of submillimeter wave gyrotrons, *Proc. 3rd Int. Workshop on Strong Microwaves in Plasmas*, Nizhny Novgorod, 1997, Vol.2, 634-659.
22. N. Miyoshi, N. Ito, I. Ogawa and T. Idehara, Combination treatment of hyperthermia and photodynamic for experimental tumor model using gyrotron (107, 203 GHz), *Proc. 35th Int. Conf. on Infrared, Millimeter and Terahertz Waves*, Italy, Th-P.11 (2010).
23. S. P. Sabchevski, T. Idehara, S. Ishiyama, N. Miyoshi, T. Tatsukawa, A dual-beam irradiation facility for novel hybrid cancer therapy, *J. Infrared, Millimeter and Terahertz Waves* 34, 71-87 (2013).
24. R. Ikeda, Y. Yamaguchi, Y. Tatematsu, T. Idehara, I. Ogawa, T. Saito, Y. Matsuki, T. Fujiwara, Broadband continuously frequency tunable gyrotron for 600 MHz DNP-NMR spectroscopy, *Plasma and Fusion Research* 9, 1206058 (2014).
25. Y. Tatematsu, Y. Yamaguchi, T. Idehara, T. Ozeki, R. Ikeda, T. Kanemaki, I. Ogawa and T. Saito, Development of a kW Level-200 GHz Gyrotron FU CW GI with a Internal Quasi -Optical Mode Converter, *J. Infrared, Millimeter and Terahertz Waves* 33, 292-305 (2012).
26. Y. Tatematsu, Y. Yamaguchi, T. Idehara, T. Kawase, I. Ogawa, T. Saito and T. Fujiwara, Characteristics of the mode converter of Gyrotron FU CW GII radiating Gaussian beams in both the fundamental and second harmonic frequency band, *J. Infrared, Millimeter and Terahertz Waves*, 35, 517-524 (2014).
27. Y. Tatematsu, Y. Yamaguchi, T. Idehara, T. K. Kawase, R. Ichioka, I. Ogawa, T. Saito and T. Fujiwara, Development of second harmonic gyrotrons, Gyrotron FU CW GII and Gyrotron FU CW GIII, equipped with internal mode converter, *J. Infrared, Millimeter and Terahertz Waves*, 35, 169-178 (2014).
28. Y. Tatematsu, Y. Yamaguchi, T. Kawase, R. Ichioka, I. Ogawa, T. Saito and T. Idehara, Analysis of oscillation characteristics and optimal condition for high power operation on Gyrotron FU CW GIII, *Physics of Plasmas* 21, 083113-1~6 (2014).
29. O. Dumbrajs, T. Idehara, T. Saito and Y. Tatematsu, Calculations of Starting Currents and Frequencies in Frequency-Tunable Gyrotrons, *Japanese Journal of Applied Physics* 51, (2012) 126601.
30. T. Idehara, M. Pereyaslavets, N. Nishida, K. Yoshida and I. Ogawa, Frequency modulation in a submillimeter-wave gyrotron, *Phys. Rev. Letts.* 81, 1973-1976 (1998).
31. A. Miyazaki, T. Yamazaki, T. Suehara, T. Namba, S. Asai, T. Kobayashi, H. Saito, T. Idehara, I. Ogawa and Y. Tatematsu, The Direct Spectroscopy of Positronium Hyperfine Structure Using a Sub-THz Gyrotron, *J. Infrared, Millimeter and Terahertz Waves*, 35, 91-100 (2014).
32. T.H. Chang, T. Idehara, I. Ogawa, L. Agusu and S. Kobayashi, Frequency tunable gyrotron using backward-wave components, *J. Applied Physics* 105, 063304-1~4 (2009).
33. T. Idehara, A. Kuleshov, K. Ueda and E. Khutoryan, Power-stabilization of high frequency gyrotrons using a double PID feedback control for applications to high power THz spectroscopy, *J. Infrared, Millimeter and Terahertz Waves* 35, 159-168 (2014).